



## **SALT TRANSPORT IN PLASTER/SUBSTRATE LAYERS: A NUCLEAR MAGNETIC RESONANCE STUDY**

**Jelena Petkovic<sup>1</sup>, Leo Pel<sup>1</sup>, Henk P. Huinink<sup>1</sup>, Klaas Kopinga<sup>1</sup>, Rob P.J. van Hees<sup>2</sup>**

### **Abstract**

The performance of specially developed restoration plasters is not always as good as expected. Salt crystallization is one of the major causes of deterioration. To understand this in more detail, we have investigated how transport in a plaster depends on the underlying masonry material. The transport of moisture and salt during drying of some plaster/substrate systems has been monitored with a Nuclear Magnetic Resonance technique. Moisture and sodium contents have been measured non-destructively at different positions in the samples. The drying behaviour differed for the investigated systems, depending on differences in pore structure of plaster and substrate. For a good performance of the plaster a proper matching of the pore-size distribution of the plaster with that of the masonry is required.

### **Key Words**

Salt crystallization, plasters, weathering, NMR.

### **1 Introduction**

The choice of restoration plasters, suitable for long-time protection, is a delicate conservation problem. The performance of specially developed plasters is not always satisfactory (Wijffels, 1997). The durability of a plaster strongly depends on its transport properties for salt and moisture. Although salt damage has been investigated intensively for several decades (Pühringer, 1983; Goudie and Viles, 1997), the mechanisms that control the formation of salt crystals in porous media are poorly understood. A better understanding of water and ion transport during drying and salt crystallization in plasters is required for understanding the salt damage and developing better plasters. The fluid transport in the single medium depends on the pore sizes (Dullien, 1991). In the present work we investigate whether large differences in the pore sizes of the plaster and the substrate influence the transport properties. In the present recommendations for the application of plasters the influence of substrate materials is not taken into account (WTA 1992).

---

<sup>1</sup> Eindhoven University of Technology, l.pel@tue.nl

<sup>2</sup> TNO Building and Construction Research, R.vanHees@bouw.tno.nl

Using NMR imaging technique we monitor quantitatively moisture and salt profiles in plaster/substrate systems. The technique is non-destructive and enables measurements of time dependent processes (i.e. drying). In the following we will explain the NMR method, and introduce the materials we used. Next, we will discuss the water transport measured during drying of these materials and the observed salt transport. Finally, we will discuss the possible consequences for salt weathering.

## 2 Experimental

The Nuclear Magnetic Resonance (NMR) imaging technique is applied for quantitative mapping of certain chemical elements in materials. Using a home-built NMR scanner, designed for the imaging of the building materials (Kopinga and Pel, 1994), we can follow the distribution of water and sodium in time during drying (Pel et al. 2002).

For obtaining the water and Na signal from a sample it is necessary to record the radio frequency (RF) signals at the resonance (Larmor) frequency of the H and Na nuclei. This frequency is determined by the magnitude of the applied magnetic field  $B$ :

$$\nu_i = \frac{1}{2\pi} \gamma_i B \quad (1)$$

where  $i$  characterizes the H or Na nucleus,  $\nu_i$  denotes the Larmor frequency and  $\gamma_i$  is the gyromagnetic ratio of the nucleus ( $\gamma_H/2\pi = 42.58$  MHz/T;  $\gamma_{Na}/2\pi = 11.27$  MHz/T). In a homogeneous magnetic field  $B$  all the nuclei of a certain type are at resonance, and a signal from the whole sample is obtained. To obtain spatial resolution it is necessary to excite the nuclei in a limited volume of the sample. The resonance frequency is made position dependent with an additional magnetic field gradient  $G$ :

$$B = B_0 + Gx \quad (2)$$

where  $x$  is a position in the sample along the direction of the magnetic field gradient  $G$ . The intensity of the received signal is proportional to the density of the nuclei  $\rho$ , which enables a quantitative analysis:

$$S = k\rho \cdot \left[ 1 - \exp\left(-\frac{TR}{T_1}\right) \right] \cdot \exp\left(-\frac{TE}{T_2}\right) \quad (3)$$

In this equation  $k$  is proportionality constant,  $T_1$  and  $T_2$  are physical parameters (nuclear relaxation times), and  $TR$  and  $TE$  are experimental parameters (Callaghan, 1991; Slichter, 1990).

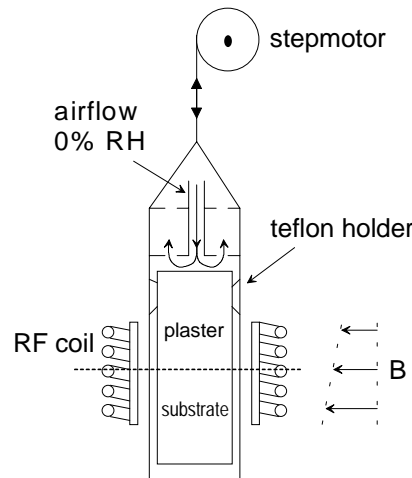


Figure 1. Set-up for drying experiments.

The main magnetic field ( $B_0$ ) and the field gradient ( $G$ ) were 0.7 T and 0.33 T/m, respectively. The resulting spatial resolution was 0.8 mm for H and 3 mm for Na. To measure the H and Na profiles over the whole sample, the sample was moved in the x direction by a step-motor (figure 1). With our equipment is possible to measure H and Na quantities in the liquid phase. During the experiment the RF frequency is switched in such a way that the H and Na signal can be recorded quasi-simultaneously (Pel, 1995; Pel et al. 2000).

The cylindrical samples had a diameter of 19 mm and a total length of 50 mm. They were sealed on all sides except at the top (the air/plaster interface). Therefore, the drying and salt transport can be considered as one-dimensional (1D) processes. Dry air is blown over the top of the sample (figure 1). The air flow was 0.7 l/min.

Experiments were done on two different plaster-substrate systems. Bentheimer sandstone and calcium-silicate brick are used as substrates. The plaster was lime based (lime:cement:sand = 4:1:10 (v/v)). These materials were selected because of the significant differences in pore-size distributions (table 1). The pores of the plaster are an order of magnitude smaller than those of Bentheimer sandstone and larger than the nano-pores of the calcium-silicate brick. Initially all samples were saturated with pure water or a NaCl solution.

*Table 1. Pore sizes measured by mercury-intrusion porosimetry.*

Material	nano-pores	micro-pores	volume ratio
Bentheimer sandstone	—	(40 ± 20) μm	—
Calcium-silicate brick	(20 ± 10) nm	(20 ± 10) μm	1:1
Plaster	—	(0.7 ± 0.4) μm	—

### 3 Results

#### 3.1 Water transport during drying

First, we have studied the drying behaviour of plaster/substrate systems saturated with pure water. In all studied cases the water evaporates from the sample through the air/plaster interface ( $x=0$ ). In figure 2 the water profiles of the Bentheimer/plaster system are plotted for different stages of the drying process. This figure shows that Bentheimer sandstone dries faster than the plaster. During the first 4 to 6 hours of the drying process the sandstone dries homogeneously, whereas the plaster remains saturated. It starts to dry when the water content in the Bentheimer sandstone is around 25% of its initial value.

In figure 3 we present the amount of water in the various layers of the plaster/Bentheimer sandstone system during the drying process. This figure confirms that during the first 5 hours only the Bentheimer sandstone dries, while the plaster stays completely saturated.

This drying behaviour can be understood as follows. During drying water tends to remain in the pores with the highest capillary pressures,  $P_c$ , which are the smallest pores according to Laplace's equation (Dullien, 1991):

$$P_c \approx \frac{2\gamma}{r} \quad (4)$$

In this equation  $\gamma$  is the surface tension of the air-water interface, and  $r$  is the pore radius.

The penetration of air in pores filled with water is only possible when the pressure difference between air and water exceeds the capillary pressure. Therefore, the resistance against air invasion is the smallest in the widest pores. Bentheimer sandstone has bigger pores than the plaster (table 1) and therefore dries first.

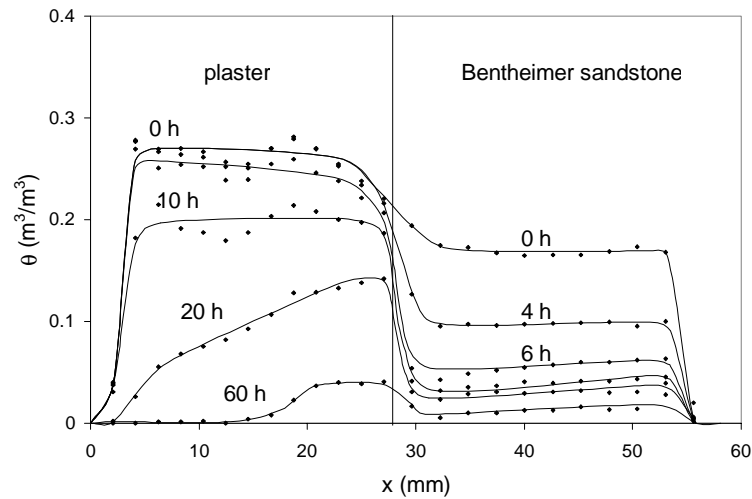


Figure 2. The water distribution in the plaster/Bentheimer sandstone system during drying. The Bentheimer sand-stone clearly dries faster than the plaster. The solid curves are drawn as guide to the eye.

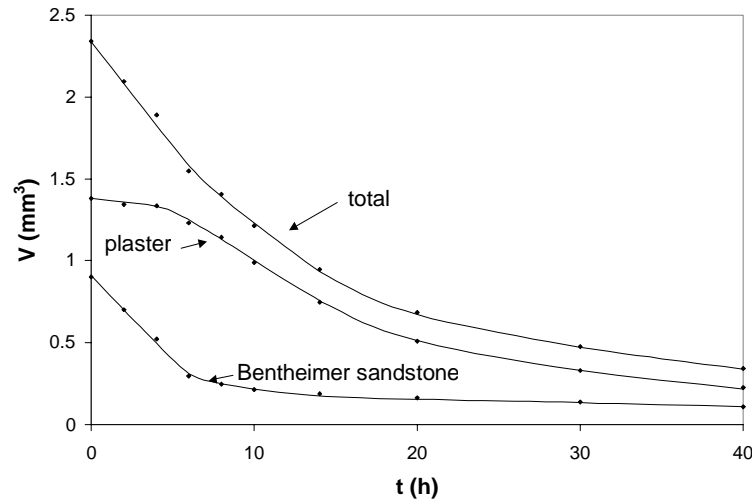


Figure 3. The amount of water in the various layers of the plaster/Bentheimer sandstone system during drying.

The plaster/calcium-silicate brick system behaves quite differently than plaster/Bentheimer sandstone system (figures 4 and 5). Initially the brick and the plaster dry simultaneously. However, between 4 and 40 hours after the start of the drying process, the calcium-silicate brick dries much slower than the plaster. After 40 hours the plaster has become almost dry, but after 150 hours a significant amount of water is still present in the brick.

This behaviour is a consequence of the two dominant pore sizes present in the calcium-silicate brick. These pore sizes are an order of magnitude bigger and smaller, respectively, than the dominant pore size of the plaster (table 1). During the first 4 hours of drying, water evaporates from the bigger pores of the brick. Also the plaster dries to some extent. The most important feature of the drying process is that after a sufficiently long time (150 h) the small pores of the brick still contain water, while the plaster is nearly dry. Again, this can be explained from the capillary pressure (eq. 4).

Air invades the widest pores, which are, at this stage of the drying process, only available in the plaster layer.

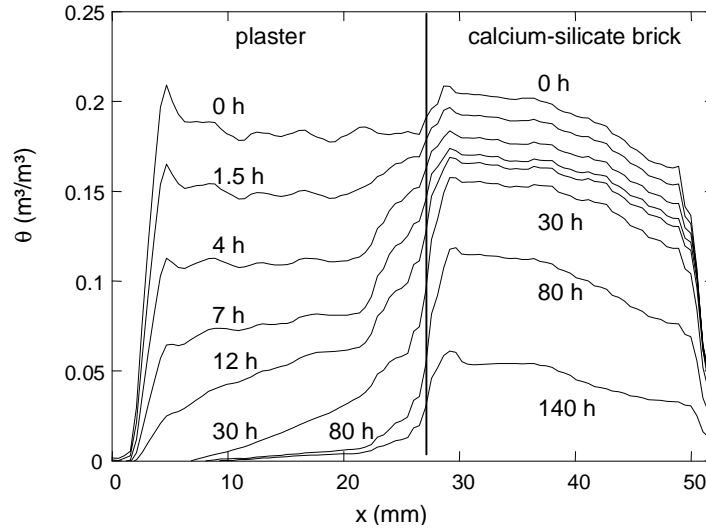


Figure 4. Water distribution in the plaster/calcium-silicate brick system during drying. The plaster dries faster than the calcium-silicate brick.

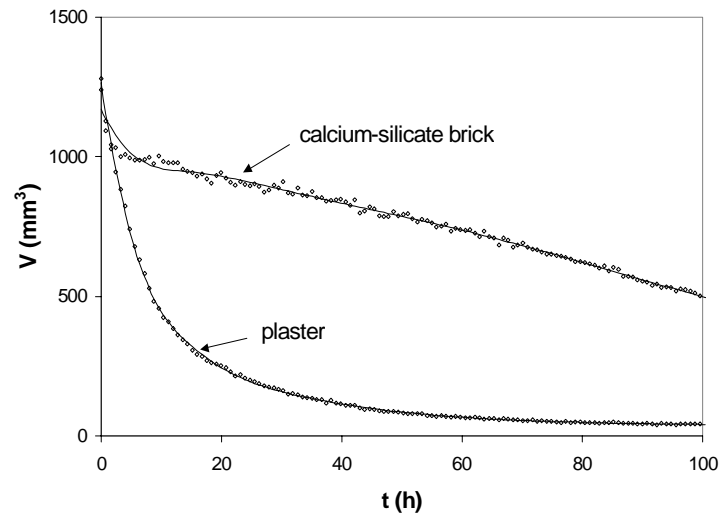


Figure 5. The amount of water in the various layers of the plaster/calcium-silicate brick system during drying.

Our drying experiments demonstrate that a certain plaster layer behaves completely different, depending on the substrate. Since in both cases considered above the plasters are the same, we can conclude that the substrate is of great importance for the transport behaviour in a plaster. The observed difference in water transport may also influence the salt transport and crystallization.

### 3.2 Salt transport and crystallization during drying

We have studied the combined transport of water and salt in the plaster/Bentheimer system. The sample was initially saturated with a 4M NaCl solution. The water profiles are presented in figure 6. The sample dries in a similar way as in the case of pure water (figure 2). The corresponding Na<sup>+</sup> concentration profiles are shown in figure 7. In connection with the water transport, differences in the salt transport in the plaster and

the Bentheimer sandstone can be observed. During the first 16 hours the salt in the Bentheimer sandstone remains uniformly distributed. The NaCl concentration does not exceed the initial concentration of 4 M. The data points show a rather large scatter, due to the low NMR signal from the Na nuclei. During drying of the Bentheimer sandstone, the amounts of H<sub>2</sub>O and Na in the liquid phase decrease and the signal to noise ratio decreases. In the plaster the salt concentration increases from 4 M to 6 M (the saturation concentration). The NaCl distribution in the plaster is not uniform, but a concentration peak develops at the drying surface. At this stage, crystallization at the air/plaster interface is visually observed.

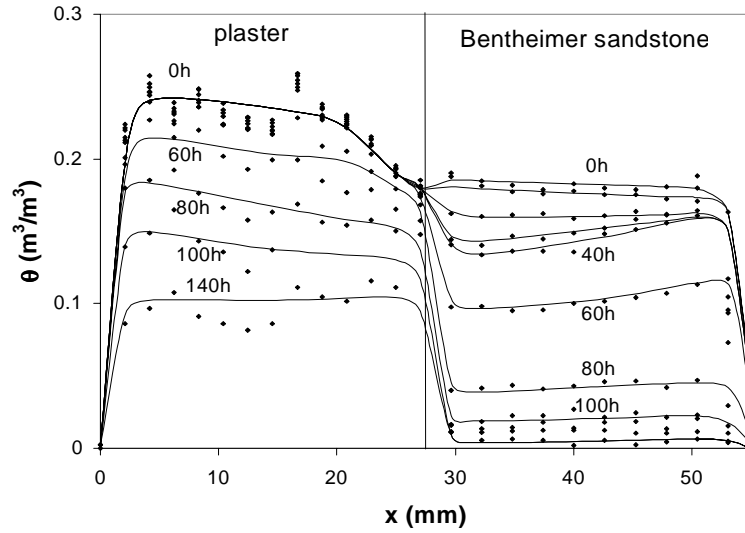


Figure 6. The water distribution in the plaster/Bentheimer sandstone system during drying. The solid curves are drawn as guide to the eye. The drying behavior is similar as in the case of pure water.

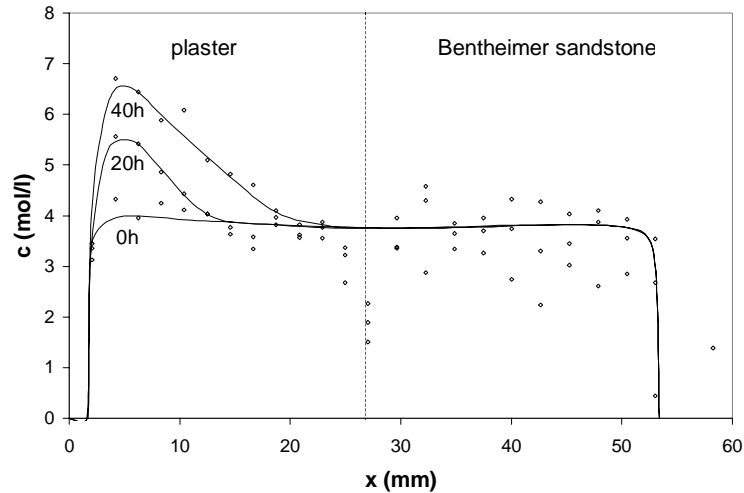


Figure 7. The NaCl concentration ( $c$  [mol/l]) in the plaster/Bentheimer sandstone system during drying. The solid curves are drawn as guide to the eye.

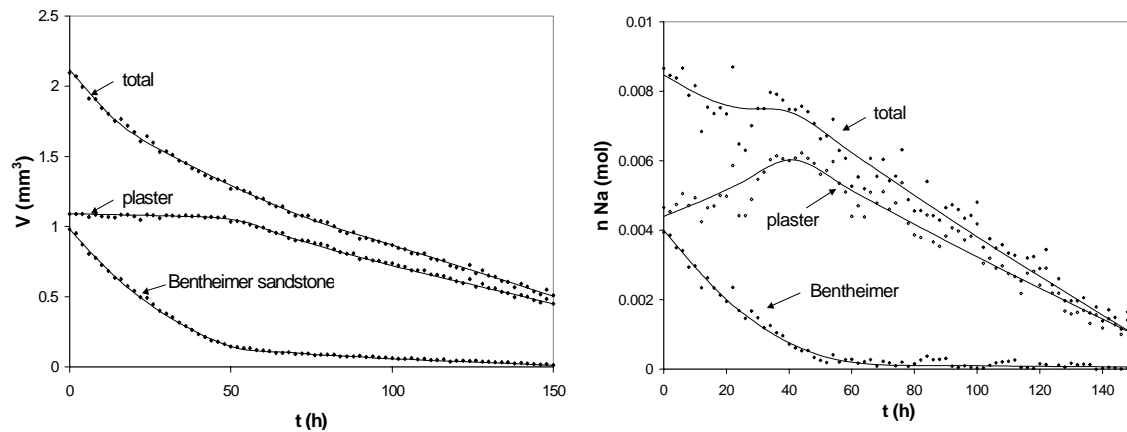


Figure 8. The amounts of water and dissolved sodium in the plaster/Bentheimer sandstone system during drying. The solid curves are drawn as guide to the eye.

The salt transport characteristics are visualized in figure 8, where we have plotted both the amount of water and the amount of dissolved sodium in the plaster/Bentheimer sandstone system during drying. Two drying stages are observed. During stage 1 (first 50 hours of drying), the Bentheimer sandstone dries and the plaster remains saturated. At the same time the amount of dissolved salt in Bentheimer sandstone decreases, and in the plaster it increases. The concentration of salt in the Bentheimer sandstone is constant within experimental inaccuracy (figure 7). Therefore, we can conclude that the salt is moving from the Bentheimer to the plaster. Due to this transport the amount of dissolved salt in the plaster increases, resulting in the observed concentration peak, see figure 7. During stage 2 the plaster dries. The amount of dissolved salt in the plaster decreases due to crystallization. Therefore, we can conclude that salt accumulates and crystallizes in the plaster layer.

## 4 Conclusions

We have shown that NMR imaging is a useful technique for non-destructive measuring of salt and water profiles in building materials during drying. Systems with the same plaster applied on a different substrate showed different drying behaviour, which we explained by differences in the pore sizes between the plaster and the substrate. The layer with the largest pores dries first. Therefore, the drying behaviour of a plaster/substrate layer depends on the pore size distributions of both the plaster and the substrate.

Measurements on salt loaded systems indicate that the salt transport and accumulation is connected to the drying behaviour of the plaster/substrate system. When the plaster has small pores compared to the substrate, most salt accumulates in the plaster. Salt transport is investigated only for the plaster/Bentheimer system, which corresponds to this situation. In the case that the plaster has the widest pores, we expect that a significant amount of salt will crystallize within the substrate itself. In this particular case the plaster dries first and the substrate stays wet. Most of the salts present in the substrate will be deposited at the plaster/substrate interface. To confirm this prediction, salt transport experiments on the plaster/calcium-silicate system are planned.

## Acknowledgements

The authors thank T.J. Wijffels (TNO) for the sample preparation, M.R. de Rooij (TNO and TU Delft) for the pore-size measurements by mercury-intrusion porosimetry. Part of this work is supported by the Dutch Technology Foundation (STW) and the EU project "COMPASS".

## References

- Callaghan, P.T., 1991, Principles of Nuclear Magnetic Resonance Microscopy, Oxford: Clarendon Press.
- Dullien, F.A.L., 1991, Porous media; Fluid transport and pore structure, 2nd ed. London: Academic Press.
- Goudie, A., Viles, H., 1997, Salt weathering hazard, Chichester: John Wiley & Sons.
- Kopinga, K., Pel, L., 1994, One-dimensional scanning of moisture in porous materials with NMR, Rev. Sci. Instrum, 65, 3673-3681.
- Pel, L., 1995, Moisture transport in porous building materials, Ph.D. thesis, Eindhoven University of Technology, Eindhoven, The Netherlands.
- Pel, L., Huinink, H.P., Kopinga, K., 2002, Ion transport and crystallization in inorganic building materials as studied by nuclear magnetic resonance, Appl. Phys. Lett, 81, 2893-2895.
- Pühringer, J., 1983, Salt desintegration, salt migration and degradation by salt – a hypothesis, Swedish Council for Building Research, Document D15. Stockholm: Spånbergs Tryckerier AB.
- Slichter, C.P., 1990, Principles of Magnetic Resonance, Berlin: Springer.
- Wijffels, T.J., Groot, C.J.W.P., Van Hees, R.J.P., 1997, Performance of restoration plasters, Proc. 11<sup>th</sup> International Brick/Block Masonry Conference, Shanghai, 1050-1062.
- WTA 1992, WTA Merkblatt 2-2-91 – Sanierputzsysteme, Wissenschaftlich technischen Arbeitsgemeinschaft für Bauwerkserhaltung und Denkmalpflege e.V. Bautenschutz und Bausanierung, 15, 59-63.